Grain boundaries and interfaces in Y-Ba-Cu-O films laser deposited on single-crystal MgO

T. S. Ravi, D. M. Hwang, R. Ramesh, Siu Wai Chan, L. Nazar, C. Y. Chen,
A. Inam, and T. Venkatesan
Bellcore, Red Bank, New Jersey 07701
(Received 25 April 1990; revised manuscript received 30 July 1990)

Y-Ba-Cu-O thin films were deposited on [001] MgO using pulsed laser deposition. The films are granular with the *c* axis normal to the surface and the *a-b* axes locked into several preferred orientations. The grain sizes range from a few hundred to a few thousand nanometers. The misorientation of the Y-Ba-Cu-O grains with respect to the MgO could be predicted by a modified version of the coincident site lattice theory, where near coincidence as opposed to exact coincidence is sought. The resulting boundaries between adjacent Y-Ba-Cu-O grains were found to be dominated by four types of low-energy boundaries, namely, low-angle, special crystallographic, near special crystallographic, and high-angle noncrystallographic boundaries. The critical current observed in this material is as high as 5×10^5 A cm^{-2} at 77 K and is believed to be a result of clean, low-energy boundaries with a high density of connected Cu-O-Cu bonds in adjacent Y-Ba-Cu-O grains.

I. INTRODUCTION

One of the most important applications of high-temperature superconducting cuprates is likely to be in the area of microelectronics, which requires the superconductors to be prepared in a thin-film form with a high degree of reliability. The quality of a superconducting thin film depends on the deposition technique, the processing condition for that deposition technique, and most importantly the substrate used.[1] Films of $YBa_2Cu_3O_{7-x}$ (hereafter referred to as Y-Ba-Cu-O) with excellent T_{c0} (critical temperature with zero resistance) and J_c (critical current density) have been grown successfully by various techniques such as laser deposition,[2] sputtering,[3] and electron beam evaporation[4] on perovskite substrates such as $SrTiO_3$.[5] The microstructure of these films has been studied by cross-sectional transmission electron microscopy (TEM) and attempts have been made to correlate the microstructure to the observed T_{c0} and J_c.[1,5] Defects observed in the microstructure of thin film Y-Ba-Cu-O are a combined result of processing conditions and the substrate used. Typically observed defects are structural edge dislocations, stacking faults, translational boundaries, and in some case where the lattice match between the substrate and Y-Ba-Cu-O is poor, one also sees grain boundaries.[6,7]

An important criterion for choosing the substrate for thin-film epitaxial growth is a good lattice match between the substrate and the thin film. For this reason, various perovskite materials such as single crystals of $SrTiO_3$, $LaAlO_3$, and $LaGaO_3$ were the commonly used substrates and have been demonstrated to produce high-J_c films. All these substrates have a lattice mismatch with the *a-b* axes of Y-Ba-Cu-O of less than 2%. There are however disadvantages in using these substrates, the main one being that they are quite expensive and are available only as small wafers (less than 2 in. in diameter). Some of the substrates are also twinned at room temperature which may result in macroscopically inhomogeneous Y-Ba-Cu-O films not suitable for patterning into microcircuits. Another disadvantage of these materials and with $SrTiO_3$ in particular is that they have high dielectric constants and high dielectric losses. Hence they are not useful for microwave applications. These drawbacks have led researchers to explore other materials as potential substrates. Of these, MgO being relatively inexpensive and having favorable dielectric properties, has attracted considerable attention.[1]

Recently we reported on the nature of the interface between the Y-Ba-Cu-O thin film grown by pulsed laser deposition on a MgO [001] substrate.[6,7] The Y-Ba-Cu-O film exhibits a polycrystalline structure with the *a-b* axes locked into several preferred orientations with respect to the substrate while maintaining the *c* axes normal to the substrate. It was noted that the lattice mismatch of 2.29% between Y-Ba-Cu-O and MgO for one of the observed orientation relationships, [010]MgO||[110]Y-Ba-Cu-O, was accommodated over a long range by the formation of periodic misfit dislocations.[7] Similarly polycrystalline structure was observed in Y-Ba-Cu-O deposited on MgO by electron beam coevaporation,[8] thermal coevaporation,[9] and magnetron sputtering.[10] However, there has been no detailed crystallographic analysis of the possible locking orientations between Y-Ba-Cu-O and the substrate. Despite the polycrystalline nature, T_{c0} as high as 90 K and J_c as high as 1×10^6 *A* cm^{-2} at 77 K have been obtained.[10] A major objective of this paper is to examine the role of the substrate in forming the grain boundaries in Y-Ba-Cu-O and its consequence on the transport properties.

The importance of grain boundaries in limiting the critical current density of the thin film has been illustrated through the work of Dimos *et al.*[11] where the critical current in films of Y-Ba-Cu-O grown on $SrTiO_3$ bicrystal substrates were measured as a function of their relative misorientation. They found that J_c was a monotonically

decreasing function of the misorientation up to an angle of $\sim 10°$ after which it became more or less constant. At this misorientation the J_c had already dropped by a factor of ~ 50. The high-angle grain boundary was therefore established as an important weak link in the current carrying capacity of Y-Ba-Cu-O. However, if this were always the case, then the superb transport properties observed in polycrystalline Y-Ba-Cu-O films on MgO substrates cannot be understood. In this paper we point out that some high-angle grain boundaries are crystallographically special boundaries (as determined by coincident site lattices) and they need not affect the transport properties in the same manner as other nonspecial boundaries. We identify the various possible orientation relationships between Y-Ba-Cu-O and MgO using TEM from planar and cross-sectional samples and compare the results to the theoretical predictions based on near-coincident site lattices between the two materials. The resulting nature of boundaries in adjacent Y-Ba-Cu-O grains are also investigated for their crystallographic speciality. Based on these observations, qualitative explanations are furnished for the observed high critical current in this polycrystalline film.

II. EXPERIMENTAL PROCEDURES

Y-Ba-Cu-O films were *in situ* deposited on single crystal [001]-oriented MgO by pulsed laser deposition. The deposition technique has been described in detail elsewhere.[2] Briefly, a 248-nm KrF excimer laser was fired at 6 Hz onto a rotating target of sintered superconducting bulk Y-Ba-Cu-O at a background O_2 pressure of 100 mTorr. The substrate holder was maintained at 830°C during deposition, with the film temperature estimated to be ~ 100°C lower. TEM planar samples were prepared by mechanical thinning, dimpling, and argon ion milling with liquid nitrogen cooling from the MgO side. TEM vertical cross-sectional samples were prepared by gluing two wafers with film side face to face, followed by mechanical polishing, dimpling, and argon ion milling to electron transparency with liquid nitrogen cooling.[12] Ion milling was carried out in a VCR ion miller which was equipped with an ion terminator for detecting perforations in optically transparent specimens. The samples were studied in a JEOL-4000FX TEM operating at 400 kV. High resolution lattice images and diffraction patterns were obtained from the cross-sectional samples along the MgO [100] zone axis. Planar views and diffraction patterns along the MgO [001] zone axis were obtained from the planar samples. The misorientations of Y-Ba-Cu-O with MgO were directly measured from these diffraction patterns.

III. RESULTS AND DISCUSSION

A typical plot of resistivity versus temperature of the Y-Ba-Cu-O thin film obtained by a standard four-point probe is shown in Fig. 1. It can be seen that the resistivity drops steeply to near 0 at a temperature of 90 K. The J_c of this film was measured across a $20\times 50\mu m^2$ microbridge to be 5×10^5 A cm^{-2} at 77 K with no magnetic field applied.

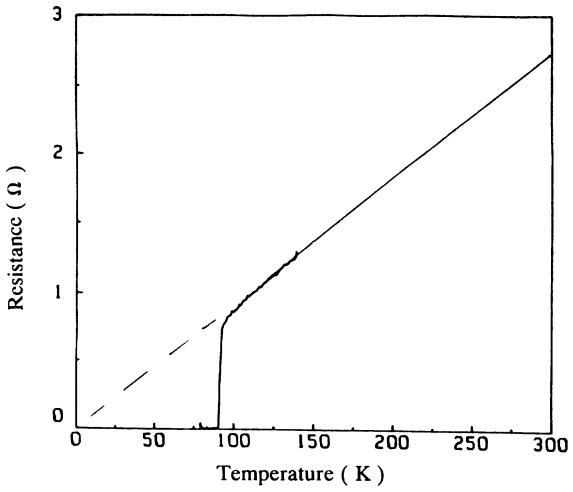

FIG. 1. Plot of resistivity versus temperature for the film of Y-Ba-Cu-O laser deposited on MgO.

Figure 2 is a typical scanning electron microscope (SEM) micrograph of the surface of the as-grown Y-Ba-Cu-O film on MgO taken with a 45° tilt from the surface normal. The surface appears to be quite smooth, the roughness estimated to be less than 0.02 μm. The elongated features present in two mutually perpendicular directions are believed to be *a-b*-axis oriented regions of Y-Ba-Cu-O in a predominantly *c*-axis-oriented matrix. The volume fraction of the (*a-b*)-oriented regions was less than 1%. The grain size of the *c*-axis-oriented regions could not be estimated from the SEM micrograph and, as will be shown later, can be easily measured from planar TEM specimens. There are also spherical particles present on the surface, a typical result of the laser ablation process. Their volume fraction in the film is also less than 1%. The dark regions on the upper left corner and the upper right of Fig. 2 are believed to be pinholes as transparent regions of similar distribution were observed in this sample by transmission optical microscopy. The presence of these pinholes in the films is insignificant; less than 0.1% of the total surface area of the film. Due to their small volume fraction, the presence of *a-b* oriented regions, the surface spherical particles, and the pinholes should have little effect on the in-plane transport properties. In this paper, therefore, we assume that the *c*-axis-oriented grains and the boundaries between these grains are the predominant microstructural characteristics that affect the transport critical current in this thin film.

The thickness of the film was measured to be 162 nm from the cross-sectional sample. The microstructure of the Y-Ba-Cu-O film was studied by cross-sectional and planar TEM. Figure 3(a), obtained from a cross-sectional sample, shows two grains of Y-Ba-Cu-O grown on MgO in a columnar manner with the *c*-layers parallel to and the grain boundary normal to the substrate surface. The lattice fringes have a faulted appearance, a typical characteristic of laser deposited films. The nature of these microfaults and their consequence on the transport

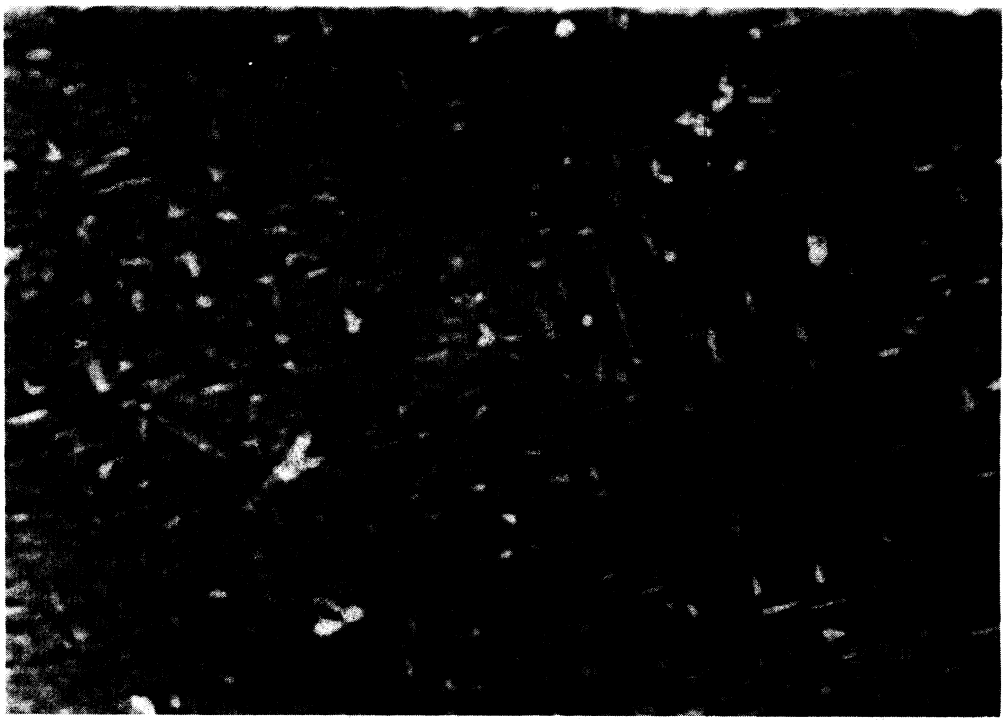

FIG. 2. Typical SEM micrograph of the surface of the as-grown film.

properties have been discussed elsewhere.[5] Figure 3(b) shows a selected area diffraction (SAD) pattern obtained from this region. This diffraction pattern was analyzed and it was found that both Y-Ba-Cu-O grains have their *c*-axes parallel to the [001]MgO axis, but different in-plane orientations. The grain on the left in Fig. 3(a) is with the [110]Y-Ba-Cu-O||[010]MgO, while the grain on the right is with [010]Y-Ba-Cu-O||[010]MgO. Thus, the misorientation between these two Y-Ba-Cu-O grains was an in-plane rotation of 45° around the common *c*-axis. Figure 3(a) also shows that there is no secondary phase at the interface and the boundary is clean.

Imaging and diffraction studies from other regions of the cross-sectional samples indicate that all the Y-Ba-Cu-O grains are with the *c*-axes parallel to the MgO [001] axis but with several preferred in-plane orientation relations. The in-plane orientation relations are difficult to establish from the cross-sectional sample, and therefore, a planar sample was used to analyze all the possible in-plane rotations. A typical planar micrograph is shown in Fig. 4. In this region, the MgO substrate has been completely removed by backside milling. The parallel features of 30–50 nm spacing are the *a-b* twinning boundaries running along the [110] direction. The twinning occurred when the sample was cooled through the tetragonal-orthorhombic transformation temperature around 450°C. At and below this temperature little crystal growth or grain boundary movement was expected. Since this paper is focused on the orientation relations between the Y-Ba-Cu-O grains and the MgO substrate which are locked in at the growth temperature before the formation of twins, in most parts of this paper we treat Y-Ba-Cu-O as a tetragonal crystal and do not differentiate [100] from [010]. From Fig. 4 we find that the grain size (not considering the *a-b* twinning) varies from a few hundred to a few thousand nanometers.

SAD patterns along the MgO [001] zone axis were obtained from many different regions in the planar sample using an SAD aperture of 0.27 μm. Figure 5 shows a diffraction pattern consisting of at least three sets of misoriented Y-Ba-Cu-O spots and the MgO spots from the substrate. The inset schematically shows the in-plane misorientations of the two dominant Y-Ba-Cu-O grains (shown by subscripts 1 and 2 in the figure) with the MgO substrate. The misorientation angles were measured to be 32° and 56° (or −34°). In this pattern, there are however other additional spots and it cannot be concluded that the two brightest sets are from adjacent grains. This type of diffraction pattern was used to search for all the possible relative misorientation angles between the Y-Ba-Cu-O grains and the MgO substrate. In some diffraction patterns, only the Y-Ba-Cu-O spots were visible (indicating that the MgO substrate had been completely removed by backside milling) and the relative misorientation of Y-Ba-Cu-O and MgO were then determined by comparing the diffraction pattern with another pattern which was obtained at the same camera length and which showed the MgO diffraction spots (such as Fig. 5). Due to the fourfold and mirror symmetry of the MgO substrate, misorientations θ, $-\theta$, and $90-\theta$ essentially represent one type of misorientation. The measured misorientations are reduced thus to $0° \leq \theta \leq 45°$ and compared with the calculated angles listed in Table I, obtained from a modified theory of the coincident site lat-

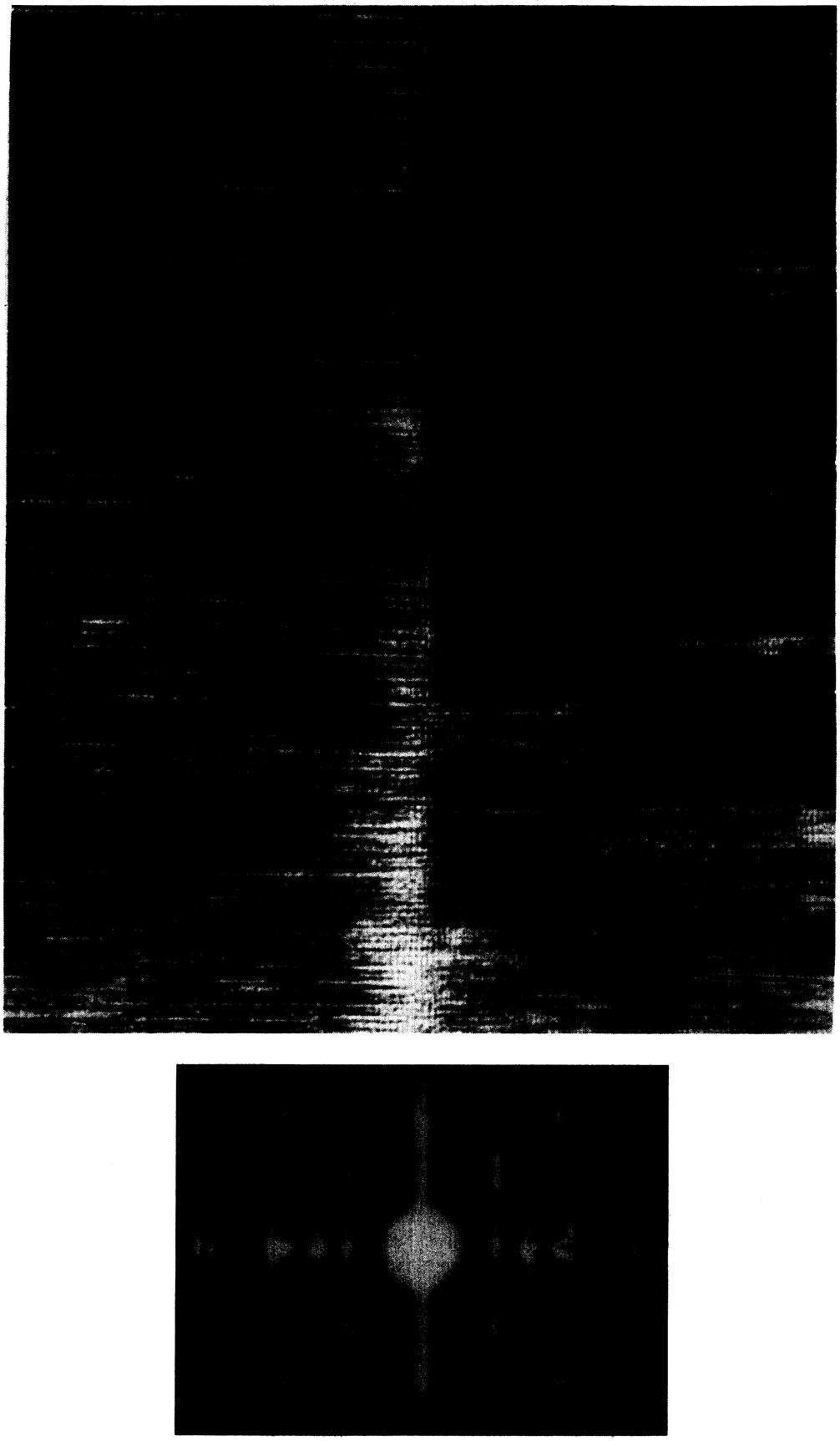

FIG. 3. (a) Cross sectional micrograph of two Y-Ba-Cu-O grains grown on MgO. (b) The diffraction pattern obtained from this region, with the primary spots indexed. Subscript *M* refers to MgO. Subscripts 1 and 2 refer to the two grains of Y-Ba-Cu-O.

FIG. 4. A typical plan view micrograph of Y-Ba-Cu-O on MgO showing different grain sizes.

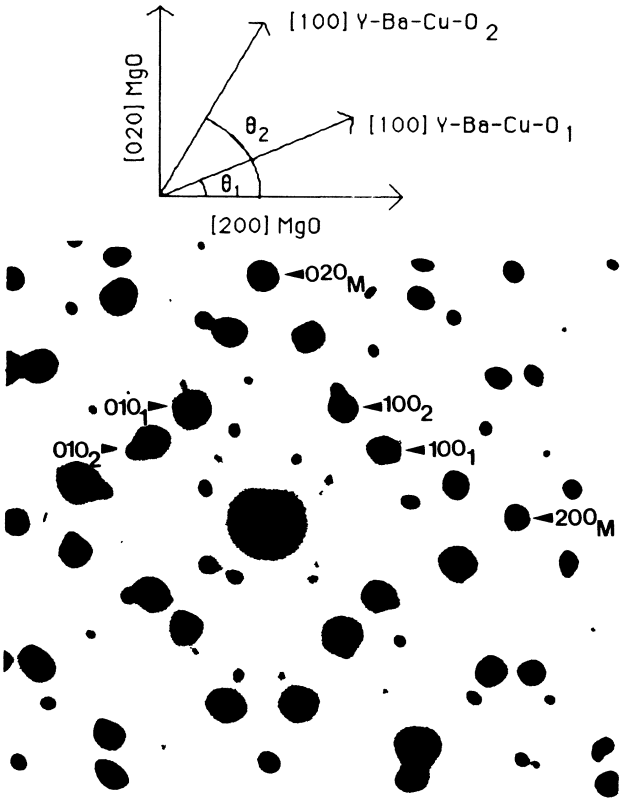

FIG. 5. A diffraction pattern obtained from the planar sample, showing spots from MgO (identified as *M*) and spots from two Y-Ba-Cu-O grains (identified as 1 and 2) superimposed. The inset is a schematic diagram showing the in-plane misorientations between the two Y-Ba-Cu-O grains and MgO (here $\theta_1 = 32°$ and $\theta_2 = 56°$).

TABLE I. Misorientation angles θ between MgO and Y-Ba-Cu-O calculated from near coincident site theory.

MgO			Y-Ba-Cu-O			Misfit	
k	l	σ_a	m	n	σ_b	δ	θ
1	0	1	1	0	1	8.89%	0°
2	0	4	2	1	5	2.97%	26.5°
4	2	20	4	3	25	2.97%	10.3°,26.5°
2	2	8	3	0	9	2.29%	45°
3	0	9	3	1	10	2.92%	18.5°
3	2	13	4	0	16	2.19%	33.7°
4	1	17	4	2	20	0.06%	12.5°,40.6°[a]
4	3	25	5	2	29	0.77%	15.1°[a],31.3°
5	0	25	5	2	29	0.77%	21.8°

[a]Denotes not observed so far.

tice (CSL).[13]

The CSL theory is modified so that near coincidence as opposed to exact coincidence is sought, allowing a mismatch in the lattices being superimposed. The method used here is also simple as we superimpose only the a-b in-plane square lattice of Y-Ba-Cu-O on the square lattice of MgO, the c-axis of Y-Ba-Cu-O being always in alignment with the MgO [001] direction. We superimpose the two square lattices with different lattice parameters and try to find out the misorientations for which a high density of near-coincident sites exists. Near-coincidence is determined by the smallness of the misfit between the different position vectors of the two lattices. It should be noted here that although the crystal structure of Y-Ba-Cu-O and MgO are different, the oxygen sublattices for these two compounds are similar, i.e., an fcc sublattice. Hence all the arguments regarding the lattice coincident sites between Y-Ba-Cu-O and MgO can be done with respect to their oxygen sublattices.

Let a be the lattice constant of MgO and b be the in-plane lattice constant of Y-Ba-Cu-O, both at the deposition temperature of 730 °C. Let k and l be the x and y coordinates of the position vectors of lattice points in MgO and let m and n be the corresponding coordinates in Y-Ba-Cu-O. Then $\sigma_a = k^2 + l^2$ is the square of the position vector $[k,l]$ for MgO and likewise $\sigma_b = m^2 + n^2$ for Y-Ba-Cu-O. The symbol "σ" is used here as opposed to the conventional "Σ" to emphasize that the lattices being superimposed are different. After superimposing the lattices, the misfits δ for various combinations of σ_a and σ_b are calculated as a percentage difference in the lengths of the position vectors with respect to their average lengths, i.e.,

$$\delta = \frac{(a\sqrt{\sigma_a} - b\sqrt{\sigma_b})}{(a\sqrt{\sigma_a} + b\sqrt{\sigma_b})/2} . \quad (1)$$

These were calculated for all possible combinations of k, l, m, and n between 0 and 6. This choice of the small position vectors ensured that the σ chosen were with a high density of lattice coincident sites and hence of low energies. We found that all the observed orientations, except the cube-on-cube case with $\theta = 0$, can be matched by choosing $\sigma_a \leq 25$ and $\delta < 3\%$. For each set of the near matched σ_a and σ_b, the misorientations (relative rotations) between the in-plane principle axes of the MgO and Y-Ba-Cu-O were calculated using

$$\theta = \tan^{-1}(l/k) \pm \tan^{-1}(n/m) . \quad (2)$$

All the misorientations were reduced to lie between 0 and 45° because, as noted earlier, of the cubic fourfold symmetry of the square lattices. Table I lists all the calculated misorientations with $\sigma_a \leq 25$ and $\delta < 3\%$ except for the $\theta = 0$ case in the first row in $\delta = 8.9\%$. Note that for each set of σ_a and σ_b, one misorientation angle is obtained if at least one of the k, l, m, and n is zero; two angles are obtained otherwise. We found that each observed misorientation matches one of the calculated values listed in Table I within the experimental error of ±0.5°. Actually, only two angles listed in Table I, 15.1° and 40.6°, have not been observed in our experiments so far. The cube-on-cube relationship of $\theta = 0°$ is the most frequently observed despite the large misfit of 8.9%. Its presence can be explained by the fact that the surface of single crystalline MgO is not atomically flat but has steps. These surface steps favor cube-on-cube epitaxy as the orientation is already fixed in two mutually perpendicular directions. The second frequently observed orientation is with $\theta = 45°$. The fact that all the observed misorientations can be accounted for by this simple geometric model indicates that those particular interfaces between Y-Ba-Cu-O and MgO are low-energy interfaces. This is not surprising because at the deposition temperature of 730°C, there is enough thermal activation in the system for it to achieve minimum energy (Y-Ba-Cu-O incongruently melts at 1350 °C).

When Y-Ba-Cu-O islands, nucleated from different sites on [001] oriented MgO surface meet, grain boundaries will be created between the adjacent Y-Ba-Cu-O grains. To examine the nature of the boundary between adjacent Y-Ba-Cu-O grains, we measured the

misorientations between many adjacent grains of Y-Ba-Cu-O from the selected area diffraction (SAD) patterns. To ensure that the diffraction patterns obtained are from adjacent grains, we used an SAD aperture of 0.27 μm diameter, and searched for patterns showing *only* spots of two superimposed square lattices. This is not an exhaustive method since many minor grain boundaries may escape detection.

It turned out that there are essentially four types of boundaries observed between adjacent Y-Ba-Cu-O grains. These boundaries are discussed in some detail in the following. The first were the low-angle grain boundaries, with in-plane misorientations between adjacent grains of less than 7°. The diffraction pattern from one such boundary is shown in Fig. 6(a). Note that patterns in Fig. 6 are presented so that the principal axes of MgO are always in the horizontal and vertical directions. Figure 6(a) represents the superposition of two Y-Ba-Cu-O diffraction patterns, rotated 26.5° and 32° with respect to the MgO substrate and thus misoriented 5.5° between themselves. The rotation angles of the two Y-Ba-Cu-O grains with respect to MgO agree with the predictions in Table I. A low-angle grain boundary structure can be described by widely spaced periodic edge dislocations. At regions away from the dislocation cores, the structural order is high and therefore the boundary energy is low. As can be seen from Table I, many combinations of θ can give rise to low-angle boundaries in Y-Ba-Cu-O. In fact, many low-angle grain boundaries were observed which is another indication of their low energy.

The second type of boundary observed was the perfect Σ twin boundary or the crystallographically special boundary. The symbol "Σ" is used as per convention to indicate boundaries in the same phase with a high degree of lattice coincidence. Figure 6(b) shows the diffraction pattern obtained from a perfect $\Sigma=5$ boundary. The angles between the two Y-Ba-Cu-O grains and the MgO were measured to be 18.5° and $-18.5°$. Therefore the orientation relationship for the two grains are as follows (as can be seen from Table I): [310]Y-Ba-Cu-O$\|$[100]MgO for one grain and [130]Y-Ba-Cu-O$\|$[100]MgO for the other grain. The misfits for

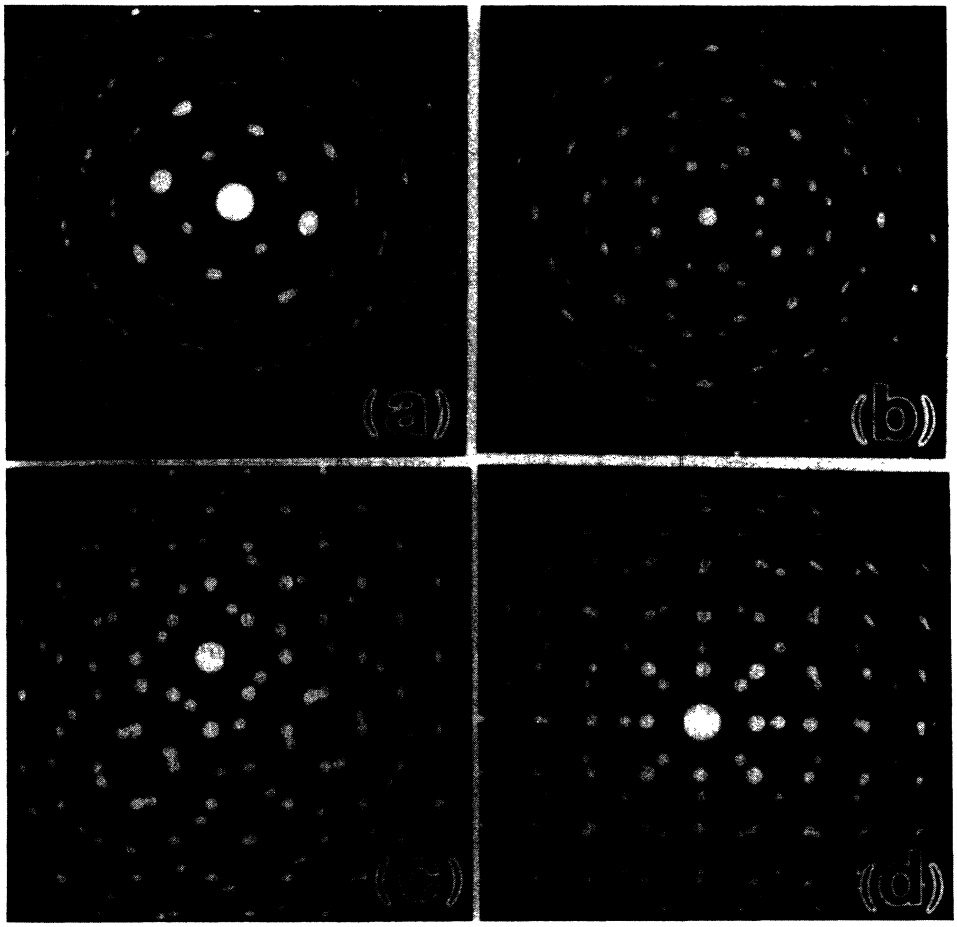

FIG. 6. Typical diffraction pattern obtained from the planar view sample for the four types of boundaries described in the text. The in-plane principal axes of MgO are in the horizontal and vertical directions in this figure. (a) Low-angle grain boundary obtained by 26.5° Y-Ba-Cu-O/MgO and 32° Y-Ba-Cu-O/MgO grains. (b) Perfect $\Sigma=5$ boundary obtained by 18.5° Y-Ba-Cu-O/MgO and $-18.5°$ Y-Ba-Cu-O/MgO grains. (c) Near $\Sigma=13$ boundary obtained by 45° Y-Ba-Cu-O/MgO and 68° Y-Ba-Cu-O/MgO grains. (d) High angle "locked-in" boundary obtained by 0° Y-Ba-Cu-O/MgO and 45° Y-Ba-Cu-O/MgO grains.

this particular misorientation between MgO and Y-Ba-Cu-O was 2.9%. The resulting two Y-Ba-Cu-O grains had a misorientation of 37°, with a perfect $\Sigma=5$ boundary between them. Perfect Σ boundaries between Y-Ba-Cu-O grains can be derived from each set of low misfit $[k,l]$ and $[m,n]$. Y-Ba-Cu-O grains may be locked into orientations making an angle $\tan^{-1}(m/n)$ and an angle $\tan^{-1}(n/m)=90°-\tan^{-1}(m/n)$ with the near-coincident position vector direction. Where grains of these two orientations meet, they automatically form a perfect $\Sigma=m^2+n^2$ boundary. These crystallographic boundaries are energetically stable as they have a uniform primary dislocation spacing in the boundary plane, which is equal to an integral number of lattice planes terminating at the interface.

The third kind of boundary is the "near Σ" locked-in boundary, with the misorientations close to a perfect Σ misorientation. An example of this is the boundary shown in Fig. 6(c) where two grains, one oriented 45° with MgO and the other oriented 68° (or −22°) with MgO are locked in. These two grains have a 23° misorientation between them which is close to 22.5°, the misorientation between two grains for a perfect $\Sigma=13$ boundary. This boundary has low energy, simply due to the fact that its misorientation is close to that of a perfect Σ boundary. This type of boundary was observed frequently as there are many misorientations of Y-Ba-Cu-O and MgO (as can be seen from Table I) which can give rise to these near Σ misorientations. According to the displacement shift complete lattice theory (DSC) of grain boundaries,[13] this type of boundary can be considered equivalent to a combination of a perfect Σ crystallographic boundary (e.g., a $\Sigma=13$ boundary) having a primary finely spaced dislocation network and a low-angle boundary, whose misorientation is the difference between the observed misorientation and the perfect Σ misorientation, and which can be represented by a secondary widely spaced dislocation network. These boundaries are also quite stable energetically.

The fourth type of boundary observed were the high-angle locked-in boundaries. Figure 6(d) shows an example of this boundary. This is the 45° boundary between a Y-Ba-Cu-O grain with a cube-on-cube $\theta=0°$ orientation with the MgO substrate, and another Y-Ba-Cu-O grain misoriented by a $\theta=45°$ with the MgO substrate. This is the same type of boundary shown in Fig. 2. The 45° boundary is not a special twinning boundary for a square lattice and its boundary energy is not a local minimum. However, the fact that this grain boundary is free from secondary phases as shown in Fig. 2 indicates that its boundary energy is still lower than twice the boundary energy of Y-Ba-Cu-O and secondary phases. Due to the nonperfect stoichiometry of the film, secondary phases are prone to be present if thermodynamically favorable.

To further illustrate the grain boundary free energy γ as a function of the misorientation Θ, we constructed the schematic diagram shown in Fig. 7. Here we use Θ to denote the relative rotation of the [001] tilt boundary between two Y-Ba-Cu-O grains, and reserved θ to denote the misorientation between a Y-Ba-Cu-O grain and the MgO substrate. Without the detailed information on the

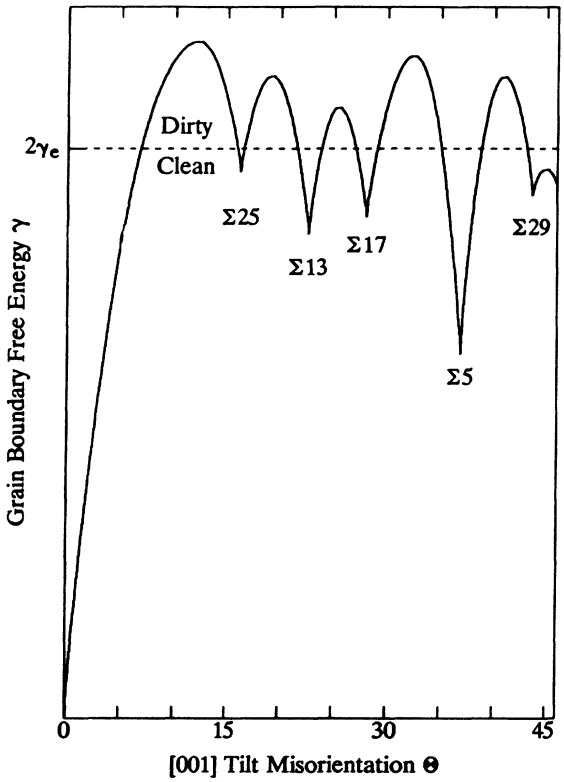

FIG. 7. A semiquantitative plot of grain boundary free energy γ versus the [001] tilt misorientation Θ. See text for details.

boundary energy, Fig. 7 was calculated following some general guidelines. (1) The boundary-free-energy γ exhibits a sharp minimum (or cusp) at each of the special c-axis tilt angle θ_i corresponding to a perfect Σ_i boundary. We considered all Σ_i's up to $\Sigma=29$. They are $\Sigma5(\theta=36.9°)$, $\Sigma13(22.6°)$, $\Sigma17(28.1°)$, $\Sigma25(16.3°)$, and $\Sigma29(43.6°)$. (2) The fraction of connected bonds in a $\Sigma_i[001]$ tilt boundary is roughly $1/\sqrt{\Sigma_i}$. Therefore, we let $\gamma(\theta)=-\gamma_0/\sqrt{\Sigma_i}$. (3) Near each of the special crystallographic angle θ_i, $\gamma(\theta)$ follows $-B|\theta-\theta_i|\ln|\theta-\theta_i|$,[14] where the parameter B was adjusted to give $\gamma(\theta)$ a reasonable appearance as shown in Fig. 7. Based on our observations we also speculate the position of the interfacial energy γ_e between Y-Ba-Cu-O and some extraneous phases and marked it in Fig. 7. If $\gamma(\theta)>2\gamma_e$, the grain boundary is likely to be decorated with some extraneous phase to lower the total free energy.

Table II summarizes the types of grain boundaries in Y-Ba-Cu-O on MgO observed in this and several other studies.[7,8,15] It is seen that all the grain boundaries observed fall into one of the four categories described above and are consistent with our semiquantitative curve of Fig. 7. Included in Table II also are the misorientations of the individual Y-Ba-Cu-O grains with respect to MgO. For the Y-Ba-Cu-O grain boundary misorientations taken from Refs. 8 and 15, the misorientations of the individual grains with respect to MgO are not reported and the

TABLE II. Dominant[a] inter-Y-Ba-Cu-O grain boundaries observed in Y-Ba-Cu-O films deposited on MgO.

Relative rotation Θ	Misorientation θ with MgO Grain 1	Grain 2	Boundary type	Diffraction pattern
4.8°	26.5°	31.3°	Low angle	Fig. 6(a)
6.5°	12.5[b]	18.5[b]	Low angle	Fig. 4 of Ref. 15
37°	18.5°	−18.5°	$\Sigma=5$	Fig. 6(b)
43.5°	21.8°[b]	−21.8°[b]	$\Sigma=29$	Fig. 3 of Ref. 15
28.5°	12.5°[b]	40.6°[b]	$\Sigma=17$	Fig. 3 of of Ref. 8
23.2°	45°	21.8°	Near $\Sigma=13$	Fig. 6(c)
45°	0°	45°	Locked-in	Fig. 6(d)
26.5°	0°	26.5°	Locked-in	Fig. 4(b) of Ref. 7
18.5°	0°	18.5°	Locked-in	Fig. 4(c) of Ref. 7

[a]Defined by the two sets of Y-Ba-Cu-O spots that were observed in a SAD pattern.
[b]In Refs. 8 and 15, only the relative rotation between the grains were reported. The misorientation angles with respect to MgO shown in this table are our speculation based on the calculation shown in Table I.

values shown in Table II are our speculation, based on the calculation shown in Table I. As can be seen readily in Table II, all the grain boundaries between adjacent Y-Ba-Cu-O grains are a result of the misorientations of the grains with the substrate.

At high temperatures, grain boundaries can move to minimize the total energy. This means that a grain may grow at the expense of its neighbors. The growth would proceed till the grain meets another grain with which it can form a low-energy boundary. If the grain it meets again happens to be unfavorably misoriented, then further grain growth would occur to rectify this situation. Such interface controlled motion has been observed in many materials.[16] The condition that is most important here is the minimization of the total boundary energy sum $\gamma_i A_i$, where γ_i is the boundary energy per unit area of the grain boundary and A_i is the surface area of each of the boundary. The planar-view micrograph of the Y-Ba-Cu-O film shown in Fig. 4 reveals grains with sizes varying from a few hundred to a few thousand nanometers, which is a few orders of magnitude higher than that expected from random nucleation of Y-Ba-Cu-O islands on the MgO surface during deposition. This and the fact that many grain boundaries form a triple point network as seen in Fig. 4, indicates that the Y-Ba-Cu-O film has gone through considerable grain boundary migration and grain annihilation.

In principle, the 16 distinct low-energy misorientations observed in the Y-Ba-Cu-O system as shown in Table I, would result in $16\times15=240$ types of Y-Ba-Cu-O–Y-Ba-Cu-O boundaries. Many of these boundaries may have high energies. However these high-energy boundaries could only exist during the initial deposition when the film thickness is negligible compared to the grain size. When the film thickness becomes comparable to the grain size, the inter-Y-Ba-Cu-O–Y-Ba-Cu-O grain boundary energy becomes important and the initial high-energy boundaries tend to move in favor of forming low-energy boundaries. Therefore the four types of low-energy boundaries shown in Fig. 5 dominate our observation with a 0.27-μm SAD aperture.

IV. CONCLUSIONS

The nature of the grain boundaries in Y-Ba-Cu-O thin films on MgO being established, it is important to relate these results to the transport properties of the film. As mentioned in the Introduction, grain boundaries have been shown to be weak links in the superconducting transport properties. Dimos *et al.*[7] predicted that, J_c across a Y-Ba-Cu-O grain boundary with a misorientation exceeding 10° is limited to 10^5 A cm^{-2} at 4.2 K or 10^4 A cm^{-2} at 77 K, independent of the intragrain J_c. However, for polycrystalline Y-Ba-Cu-O on MgO, we found the J_c to be just an order of magnitude lower than that measured on single crystal films of Y-Ba-Cu-O grown on $SrTiO_3$. A $J_c=5\times10^5$ A cm^{-2} at 77 K has been measured for the sample used in this study. Our laboratory has consistently produced Y-Ba-Cu-O films on MgO with $J_{c,77\,K}$ exceeding 10^6 A cm^{-2} using similar laser deposition conditions. $J_{c,77\,K}$ exceeding 10^6 A cm^{-2} from films on MgO has also been reported by other groups.[10]

One of the reasons for the high J_c in films on MgO is the fact that in all the Y-Ba-Cu-O grains the c planes were observed to be parallel. For the low-angle grain boundary, as observed earlier by Dimos *et al.*, there is no significantly reduction in the J_c. However, Dimos *et al.* have also suggested that the J_c at a grain boundary is primarily dependent on the structural disorder of the grain boundary.[17] This, in turn, depends only on the misorientation angle and not on the specific type of the misorientation. For example, the J_c across a [001] tilt boundary with misorientation θ in Y-Ba-Cu-O would be the same as J_c across a [100] twist boundary misoriented by the same θ. This would imply that the connectivity of the Cu—O—Cu bond directions in Y-Ba-Cu-O is not a factor in the suppression of J_c at high misorientation angles. This may not be true in the case of perfect low Σ boundaries formed around the [001] tilt axis. For this kind of a boundary, there exists a perfect one-to-one correspondence between the Cu—O—Cu bonds in the adjacent grains, the positions of such correspondence determined

by the density of coincident lattice sites. Therefore J_c is not significantly reduced across such a boundary. The same should be true for boundaries which have misorientations close to that of a perfect Σ boundary. In the plot of J_c versus the misorientation of the two grains, if we take into account these perfect Σ boundaries and near Σ boundaries, there should be inflections in the curve for these misorientations, in analogy to the curve shown in Fig. 7.

We found that, for Y-Ba-Cu-O films laser deposited on [001]MgO, the *c* planes are always parallel to the MgO (001) surface. The *a-b* axes of Y-Ba-Cu-O are locked into several preferred orientations which can be predicted by a theory based on near coincident lattice sites. The grain size varies from a few hundred to a few thousand nm. The dominant orientation is $\theta=0°$, followed by $\theta=45°$. Y-Ba-Cu-O grains, with their orientations locked-in with the substrate, in turn form low energy inter-Y-Ba-Cu-O boundaries of the four types described earlier. The microbridges used for our J_c measurements were 20 μm wide and 50 μm long. Although we cannot quantify the exact fraction of the grains with the dominant $\theta=0°$ orientation, using TEM we estimated that the $\theta=0°$ oriented grains do not exceed 73% of the total surface area and the supercurrent cannot percolate *only* through the grains of this orientation.[18] Therefore, the currents need to pass across many grain boundaries and some of them are high-angle boundaries such as $\Theta=45°$. The existence of high-angle special boundaries is also evident in the ac-susceptibility measurement shown in Fig. 1(b) of Ref. 19, taken from a similar film. The quadrature signal of this measurement exhibits several cusps between 88 and 70 K, in contrast to a single transition obtained for films deposited on $SrTiO_3$. Hence, the J_c for the high-angle grain boundaries in our films is at least 5×10^5 A cm^{-2} at 77 K, a factor of 50 higher than the prediction of Dimos *et al.*[11,17] This contradiction can be resolved by allowing a high J_c to flow across special crystallographic boundaries. The high-angle grain boundaries, studied by Dimos *et al.* with bicrystal substrates, do not include those special boundaries.

The reason for J_c suppression in Y-Ba-Cu-O films on MgO (by a factor of 10 in comparison to that on $SrTiO_3$), we believe, comes from high-angle locked-in boundaries. Those boundaries have misorientations much different from perfect Σ tilt boundaries, and the connectivity in the Cu—O—Cu bonds between the adjacent grains is lost. For example, the 45° locked-in boundary shown in Figs. 6(d) and 3(a) may reduce J_c by a factor of 10.

Some of the Y-Ba-Cu-O grains may also be locked into high-energy, high-angle boundaries which are the type of boundaries described in the work of Dimos *et al.* and may significantly reduce J_c. Some of these boundaries could also be regions of preferred chemical segregation of secondary phases which cause further suppression of the J_c. However, those boundaries, having high energy, are unstable under grain boundary migration. Their presence is insignificant in our films and escaped our SAD observation. Therefore, their role in reducing J_c in our films is not important.

In summary, it was found that interfaces in Y-Ba-Cu-O films laser deposited on MgO are specific interfaces and could be predicted by the theory of near-coincident lattice sites. The resulting boundaries observed between Y-Ba-Cu-O grains were low angle, perfect Σ, near perfect Σ, or low-energy high-angle locked-in boundaries depending both on the initial nucleation of Y-Ba-Cu-O islands on MgO as well as on grain boundary migration and grain annihilation. These grain boundaries are low energy in nature and do not significantly reduce the J_c. The presence of the high-energy locked-in boundaries, which could severely suppress J_c, is not significant in our films as a result of grain boundary migration and annihilation. Therefore, J_c of 5×10^5 A cm^{-2} at 77 K was observed in our polycrystalline film.

Note added in proof: After this paper had been accepted for publication, two related works were published. B. H. Mockley *et al.* [Appl. Phys. Lett. **57**, 1687 (1990)] reported the preparation of Y-Ba-Cu-O films on the thermally annealed MgO substrate. Thermal annealing results in surface steps on the substrate which favor cube-on-cube epitaxy of the Y-Ba-Cu-O grains. They could achieve a $J_{c,77\,K}$ of 6×10^6 A cm^{-2}. S. E. Babcock *et al.* [Nature **347**, 167 (1990)] observed weak-link free transport behavior in some high-angle grain boundaries in flux-grown Y-Ba-Cu-O that were close to Σ misorientations. This observation is quite consistent with our predictions.

[1]L. A. Teitz, C. B. Carter, D. K. Lathrop, S. E. Russek, R. A. Buhrman, and J. R. Michael, J. Mater. Res. **4**, 1072 (1989).

[2]A. Inam, M. S. Hegde, X. D. Wu, T. Venkatesan, P. England, E. W. Chase, C. C. Chang, J. M. Tarascon, and J. Watchman, Appl. Phys. Lett. **53**, 908 (1988).

[3]K. Setsune, T. Kamada, H. Adachi, and K. Wasa, J. Appl. Phys. **64**, 1318 (1988).

[4]S. W. Chan, B. G. Bagley, L. H. Greene, M. Giroud, W. L. Feldman, K. R. Jenkin, and B. J. Wilkins, Appl. Phys. Lett. **53**, 1443 (1988).

[5]D. M. Hwang, T. Venkatesan, C. C. Chang, L. Nazar, X. D. Wu, A. Inam, and M. S. Hegde, Appl. Phys. Lett. **54**, 1702 (1989).

[6]R. Ramesh, D. M. Hwang, T. Venkatesan, T. S. Ravi, L. Nazar, A. Inam, X. D. Wu, B. Dutta, G. Thomas, A. F. Marshall, and T. H. Geballe, Science **247**, 57 (1990).

[7]R. Ramesh, D. M. Hwang, T. S. Ravi, A. Inam, J. B. Barner, L. Nazar, S. W. Chan, C. Y. Chen, B. Dutta, and T. Venkatesan, Appl. Phys. Lett., **56**, 2243 (1990); D. M. Hwang, T. S. Ravi, R. Ramesh, S. W. Chan, C. Y. Chen, L. Nazar, X. D. Wu, A. Inam, and T. Venkatesan, Appl. Phys. Lett. **57**, 1690 (1990).

[8]L. A. Tietz, C. B. Carter, D. K. Lathrop, S. E. Russek, and R. A. Buhrman, in *Proceedings of the 46th Annual EMSA Meeting,* edited by G. W. Bailey (San Francisco Press, San Francisco, 1988), p. 870.

[9]P. Berberich, J. Tate, W. Dietsche, and H. Kinder, Appl. Phys. Lett. **53**, 925 (1988).

[10]Q. Li, O. Meyer, X. X. Xi, J. Geerk, and G. Linker, Appl. Phys. Lett. **55**, 310 (1989).

[11]D. Dimos, P. Chaudhari, J. Mannhart, and F. K. Legoues, Phys. Rev. Lett. **61**, 219 (1988).

[12]L. Nazar, in Proceedings of the 46th Annual EMSA Meeting (Ref. 8), p. 923.

[13]R. W. Baluffi, A. Brokman, and A. H. King, Acta Met. **30**, 1453 (1982).

[14]W. T. Read and W. Shockley, Phys. Rev. **78**, 275 (1950).

[15]M. G. Norton, L. A. Tietz, C. B. Carter, S. E. Russek, B. H. Moeckly, and R. A. Buhrman, Mat. Res. Symp. Proc (to be published).

[16]R. W. Cahn, in *Physical Metallurgy Vol. 2: Recovery and Recrystallization,* edited by R. W. Cahn and P. Haasen (North-Holland, Amsterdam, 1983), p. 1653.

[17]D. Dimos, P. Chaudhari, and J. Mannhart, Phys. Rev. B **41**, 4038 (1990).

[18]R. B. Laibowitz, R. F. Voss, and E. I. Alessandrini, in *NATO ASI Series Vol. 109: Percolation, Localization, and Superconductivity,* edited by A. M. Goldman and S. A. Wolf (Plenum, New York, 1983), p. 145.

[19]R. Ramesh, D. M. Hwang, J. B. Barner, L. Nazar, T. S. Ravi, A. Inam, B. Dutta, X. D. Wu, and T. Venkatesan, J. Mater. Res. **5**, 704 (1990).

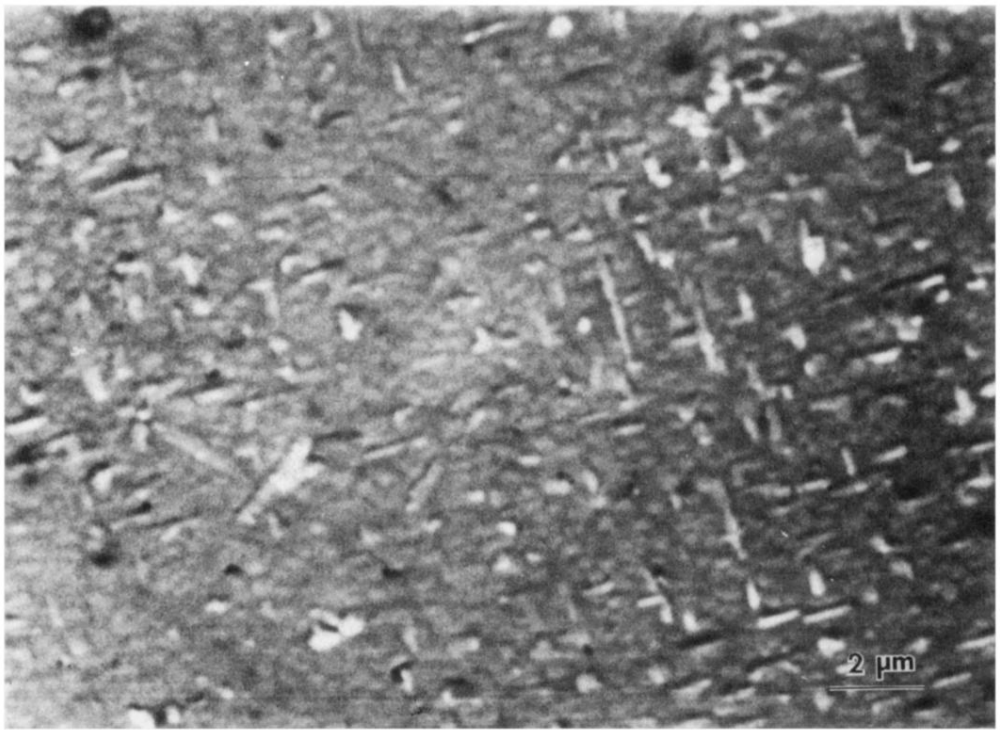

FIG. 2. Typical SEM micrograph of the surface of the as-grown film.

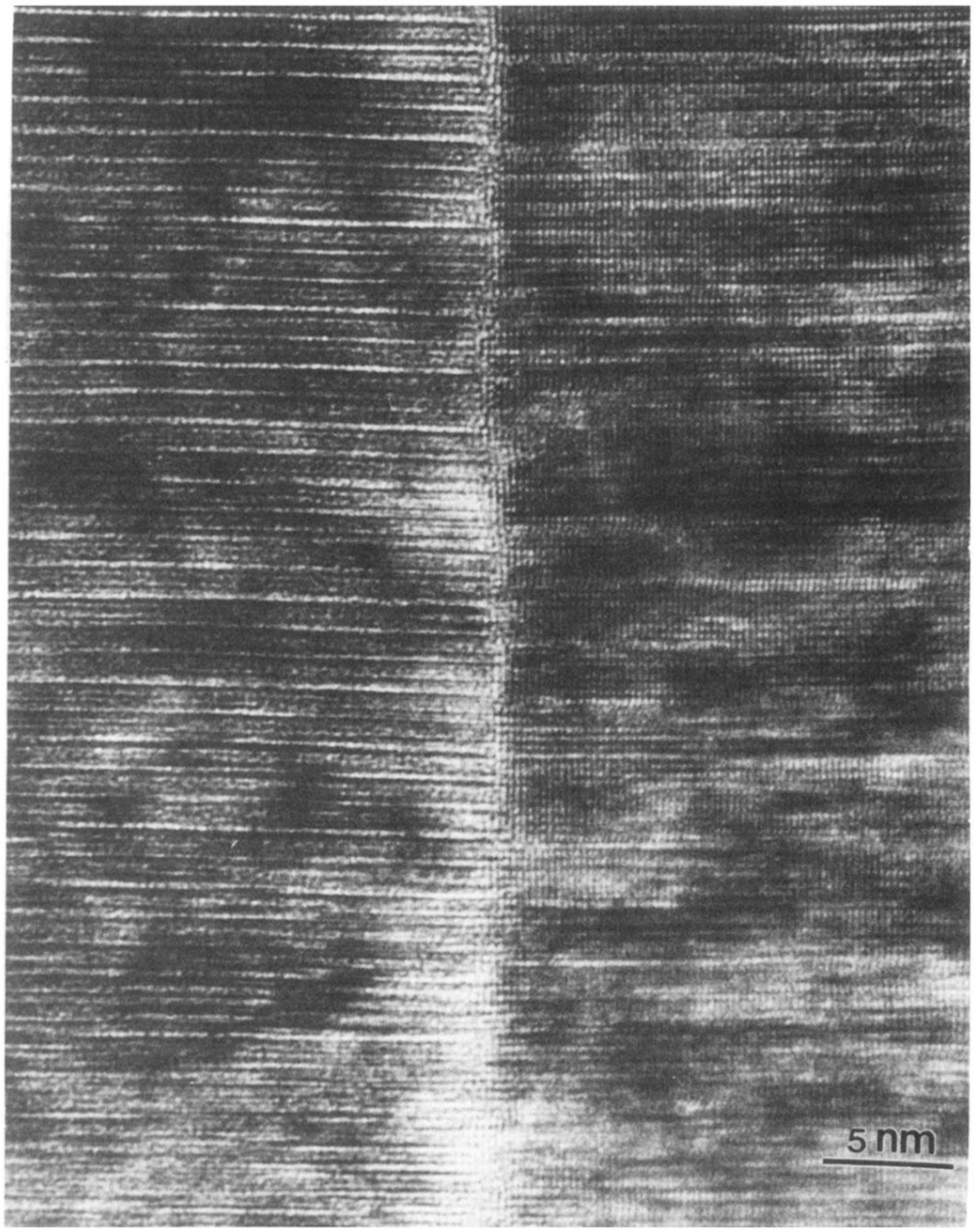

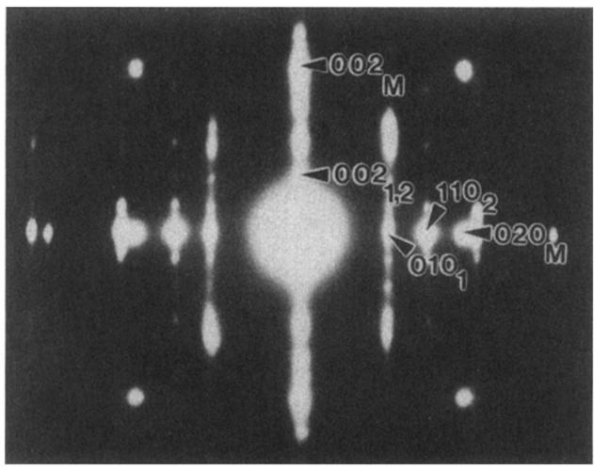

FIG. 3. (a) Cross sectional micrograph of two Y-Ba-Cu-O grains grown on MgO. (b) The diffraction pattern obtained from this region, with the primary spots indexed. Subscript *M* refers to MgO. Subscripts 1 and 2 refer to the two grains of Y-Ba-Cu-O.

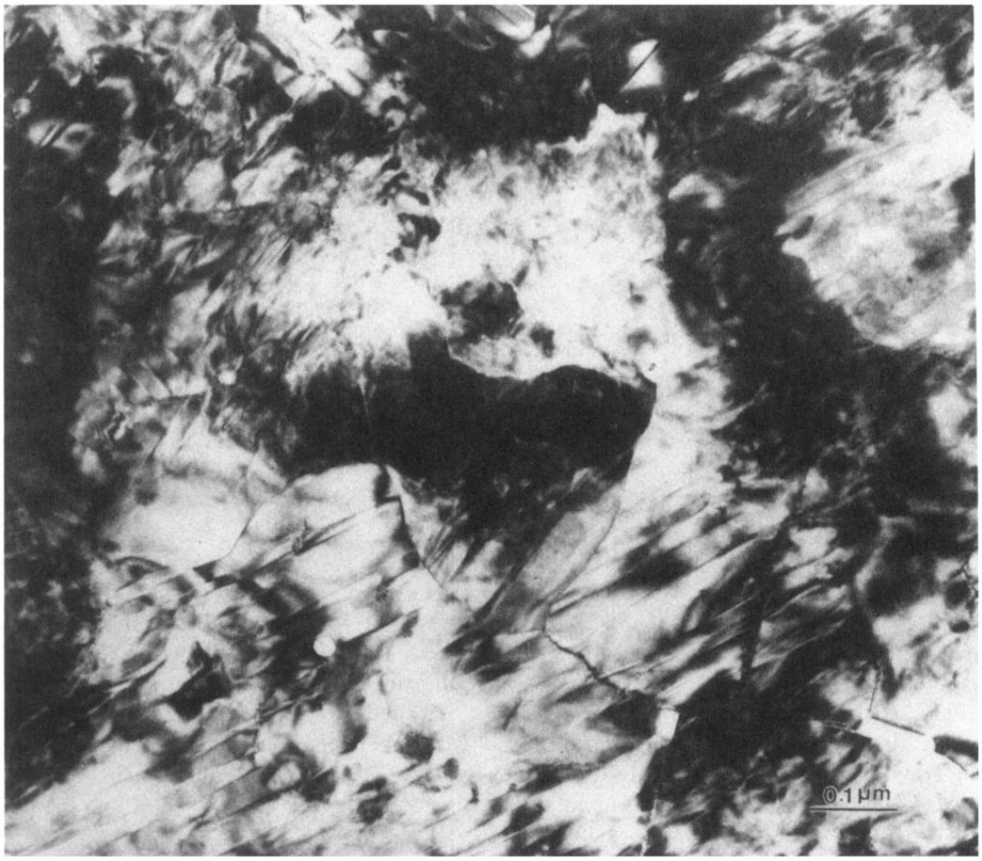

FIG. 4. A typical plan view micrograph of Y-Ba-Cu-O on MgO showing different grain sizes.

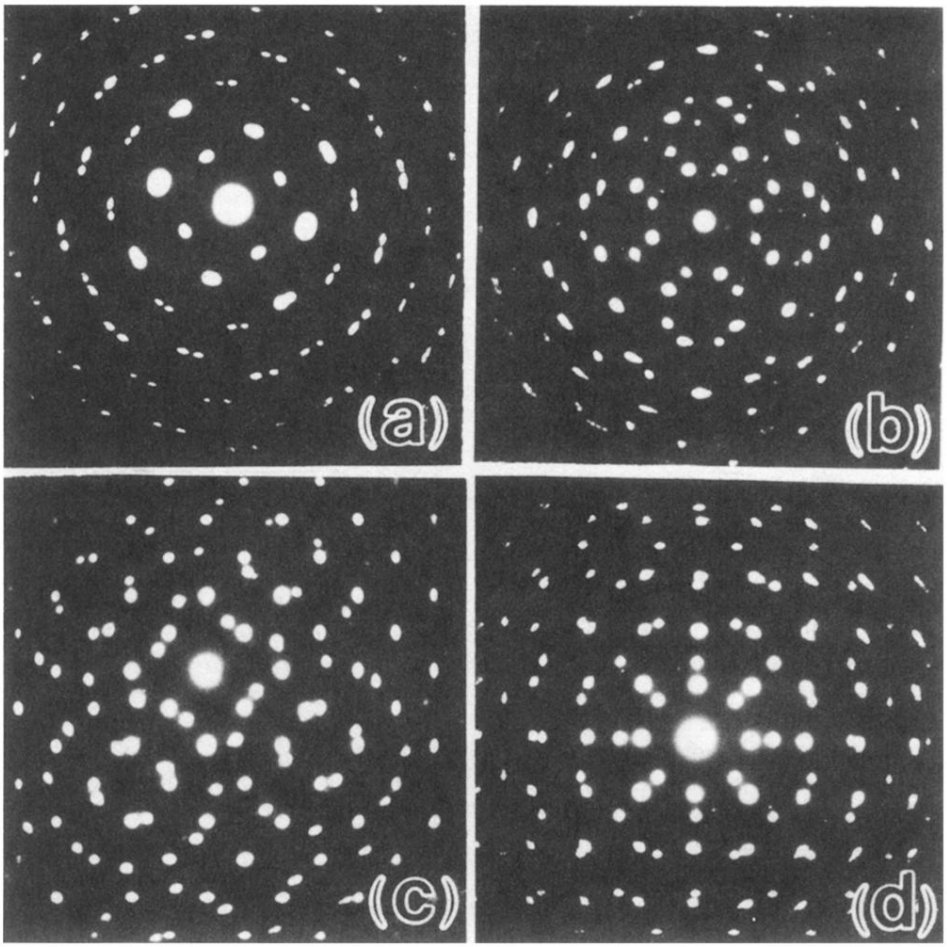

FIG. 6. Typical diffraction pattern obtained from the planar view sample for the four types of boundaries described in the text. The in-plane principal axes of MgO are in the horizontal and vertical directions in this figure. (a) Low-angle grain boundary obtained by 26.5° Y-Ba-Cu-O/MgO and 32° Y-Ba-Cu-O/MgO grains. (b) Perfect $\Sigma=5$ boundary obtained by 18.5° Y-Ba-Cu-O/MgO and $-18.5°$ Y-Ba-Cu-O/MgO grains. (c) Near $\Sigma=13$ boundary obtained by 45° Y-Ba-Cu-O/MgO and 68° Y-Ba-Cu-O/MgO grains. (d) High angle "locked-in" boundary obtained by 0° Y-Ba-Cu-O/MgO and 45° Y-Ba-Cu-O/MgO grains.